Eur. Phys. J. D **9**, 529–533 (1999)

THE EUROPEAN PHYSICAL JOURNAL D

EDP Sciences

Metallic cluster beams from a 2.5 MV Van de Graaff accelerator for cluster–solid interaction studies: preliminary results with Au_n^+ clusters

M. Fallavier[1], Y. Champelovier[1], M. Ferrari[1], R. Kirsch[1], J.C. Poizat[1], J. Remillieux[1], J.P. Thomas[1], B. Canut[2], M. Monchanin[2], S.M.M. Ramos[2], P. Thévenard[2], S. Della Negra[3], J.P. Mouffron[3], and P. Nicol[3]

[1] Institut de Physique Nucléaire de Lyon, IN2P3-CNRS, Université Claude Bernard Lyon-1, F-69622 Villeurbanne Cedex, France
[2] Département de Physique des Matériaux, UMR CNRS 5586, Université Claude Bernard Lyon-1, F-69622 Villeurbanne Cedex, France
[3] Institut de Physique Nucléaire d'Orsay, IN2P3-CNRS, F-91406 Orsay Cedex, France

Received: 31 August 1998 / Received in final form: 27 October 1998

Abstract. A liquid metal ion source (LMIS) was installed on the high-voltage terminal of the 2.5 MV single-stage Van de Graaff accelerator of the Institut de Physique Nucléaire de Lyon and was used to deliver intense MeV energy beams of cluster ions. After acceleration, the ions produced from an eutectic Au–Si alloy were mass-selected by means of a magnetic analysis. The beam was mainly composed of the monoatomic ions Au^+ and Si^+ and of the clusters Au_n^+, Au_nSi^+, and $Au_nSi_2^+$ ($n = 2 - 13$). The intensities decreased for increasing n values, but remained remarkably high. For pure gold ions, the maximum intensity measured at the target site varied from 250 nA, for Au^+, down to 20 pA, for Au_9^+. The research program on the study of the specific effects of the impact of energetic clusters on solid surfaces concerns the fundamental interaction processes and the solid modifications induced by high-density energy deposits. Our first experiments with Au_n^+ clusters led to the following results: Nonlinear dependence on the cluster size of kinetic secondary electron emission from thin carbon foil enhances the damage rate of irradiated silicon crystals as compared to monoatomic Au^+ ion effects.

PACS. 79.20.Rf Atomic, molecular, and ion beam impact and interactions with surfaces – 36.40.-c Atomic and molecular clusters – 61.80.Lj Atom and molecule irradiation effects

1 Introduction

The interaction processes of accelerated cluster ions in solids comprise a wide field of fundamental and applied research that has been the subject of growing interest in recent years [1, 2]. The impact of an energetic cluster on a solid surface can be seen as the simultaneous arrival of many ions at close distances in the solid, which gives rise to a high-density energy deposit in the solid. Subsequent processes, such as surface secondary emissions and sputtering, and material damaging, are highly modified when compared to the effects of monoatomic ion impacts. All these specific effects of energetic cluster impact on solids are commonly called cluster effects. Tandem electrostatic accelerators are now able to produce beams of various heavy atom clusters and C_{60}^+ fullerene ions with total energies ranging from 1 MeV up to a few 10 MeV. However, because tandems used in standard mode are based on ion charge exchange at the high-voltage terminal, they can deliver only reduced beam intensities for weakly bound metal clusters. In this respect, improvements can be obtained with a positive cluster ion source set in the high-voltage terminal, as has been done in the Orion facility on the 15 MV tandem of the Institut de Physique Nucléaire d'Orsay [3]. In order to produce metal cluster beams at lower energies, we installed a liquid metal ion source (LMIS), known for the production of intense ion beams, on the 2.5 MV terminal of a single-stage Van de Graaff accelerator. The total energy range, between 150 keV and 2.5 MeV, is expected to be well suited for studies of the physical processes occurring during cluster impact on a solid surface and for the structural and chemical modifications induced in solids. The reason is that in this keV/amu energy range, both collisional interactions with target atoms and inelastic interactions with target electrons contribute to the energy deposit in the solid and can be studied with the same experimental facility.

In this paper, we present the characteristics of the gold cluster beams produced on the 2.5 MV Van de Graaff accelerator in Lyon and report on some results of first experiments. The cluster effects on inelastic electronic interactions and atomic collisional interactions are illustrated by measurements of secondary electron emission from thin

carbon foils and measurements of damage creation in silicon crystals, respectively.

2 MeV cluster beams

The liquid metal ion source is similar to the source of the ORION facility of the IPN d'Orsay [3] and has been designed there. To install it on the high-voltage terminal of the 2.5 MV Van de Graaff accelerator of the Institut de Physique Nucléaire de Lyon has required appropriate modifications of the terminal and the development of specific power supplies. In the LMIS source, a tungsten needle, in contact with a filament coated by an Au–Si eutectic alloy, is wetted by liquid metal when the filament and needle are heated up to the alloy melting point ($\approx 300\,^{\circ}$C) by means of a dc current. Ionization and extraction of the ions are achieved by means of a 10 kV potential difference between the heated needle and a facing electrode. The controls and data of the electronic devices in the accelerator terminal are transmitted through optical fibers connecting the control desk to the high-voltage terminal. From the injection of all the ions in the accelerating tube, a total beam current of $\approx 5\,\mu$A is measured at the tube exit. At this stage, the beams are focused by means of an electrostatic quadrupole lens and are magnetically mass-analyzed. On the 3° exit of the analyzing magnet, the beam line houses a conventional setup for ion beam monitoring (collimators, Faraday cups). A first target chamber, equipped with electrostatic plates for beam sweeping, allows us to perform homogeneous irradiations up to a 1 cm^2 target area with high-intensity cluster beams. After this, a second target chamber houses various particle detectors needed for coincidence experiments, such as the event-by-event detection of secondary electrons emitted upon cluster impact on solid targets, and for a precise monitoring of the incident clusters. These experimental setups are described below. The residual pressure in the whole beam line is in the 10^{-7} mbar range.

Figure 1 shows the mass spectrum of the clusters produced from the Au–Si alloy in the LMIS source, accelerated to 1.8 MeV per charge unit and mass-selected by magnetic analysis. This spectrum was obtained for a 500 μm aperture of the defining slit at the exit of the magnet. These conditions offer a good compromise between beam intensity at the target site and mass separation of Au_n^+ and Au_nSi^+ clusters up to Au_9^+. The singly charged ions are mainly the monoatomic ions Au^+ and Si^+, and the clusters Au_n^+, Au_nSi^+, and $Au_nSi_2^+$ ($n = 2-13$). For a given n value up to $n = 9$, Au_n^+ is the most intense beam, followed by Au_nSi^+ and $Au_nSi_2^+$. For large clusters ($n > 9$), the relative abundances of the three cluster species are of the same order. The beam current decreases for increasing n values, but remains remarkably high. Current intensities are typically above 10 nA for small clusters ($n \leq 3$) and a few tenths of a pA for the largest clusters ($7 \leq n \leq 13$). Doubly charged clusters with small n values, also produced in the 1 nA range (for example 2 nA for Au_3^{++}), allow us to extend the experimental energy range up to 5 MeV.

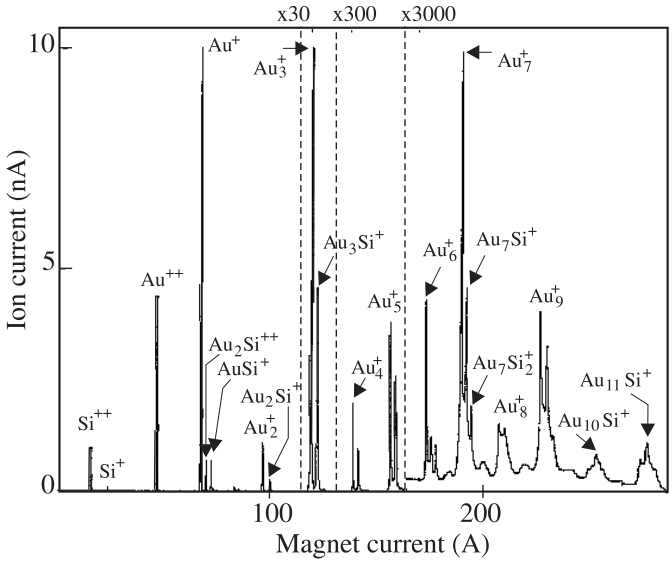

Fig. 1. Mass spectrum of the cluster ion beams produced from an Au–Si alloy in the LMIS source and accelerated to 1.8 MV per charge unit (defining slit aperture: 500 μm).

3 Cluster effect on kinetic secondary electron emission

In order to perform projectile-by-projectile secondary electron emission measurements, we tightly collimated the mass-analyzed gold cluster beam by means of two collimators of adjustable diameters (50 μm to 1 mm) located 1.7 m apart, in such a way that the beam intensity on the target was of the order of a few hundreds ions per second. Moreover, we made sure of the integrity of incident clusters by means of a transverse electric field that was applied in the region of the target when the target is off the beam: The downstream charge energy analysis revealed the possible presence of charged or neutral cluster fragments. The fraction of intact clusters was above 98% in all our measurements.

The secondary electron multiplicity was measured by means of a silicon detector facing (at ≈ 1.5 cm) the entrance surface of a thin carbon target (37 nm) tilted at 45° to the beam direction. The detector was grounded and the target was brought to a negative potential $-V_0 (V_0 = 20$ kV). In these conditions, the n electrons emitted by an incident projectile were directed to the detector, which delivered a signal corresponding to the energy neV_0. Triggering the electron detection by the detection of one (at least) atomic gold fragment transmitted through the thin target eliminated background cold emission. The electron multiplicity distributions were deduced from the energy spectra given by the electron detector by means of a fitting procedure [4, 5] that takes into account the energy resolution of the detector and the probability of each electron to be backscattered out from the detector (and to then lay down a reduced amount of energy in the detector). Only the electron yield γ_B (the mean electron number per projectile impact) will be considered here. Prior to electron measurements, the surface of the carbon target was cleaned up

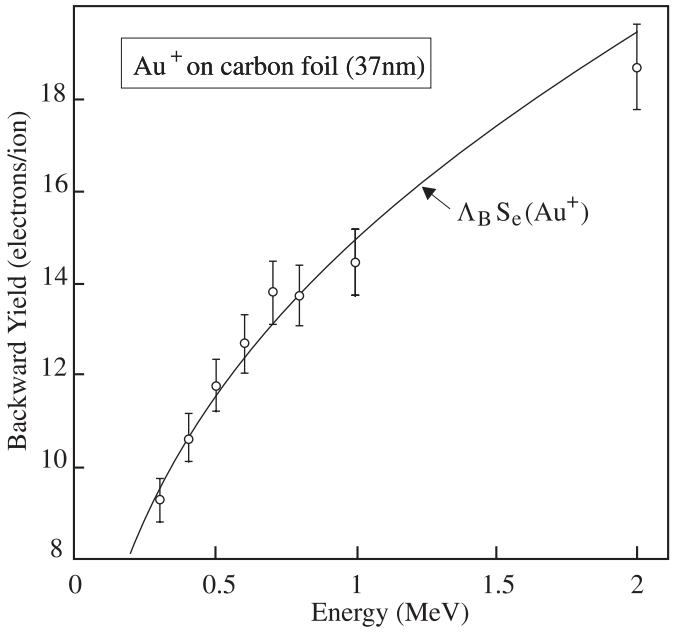

Fig. 2. Energy dependence of the backward electron yield from a carbon foil under the impact of Au^+ ions. The solid line is a fit of $\gamma_B(Au^+)$ by $S_e(Au^+)$; Λ_B is the proportionality coefficient discussed in the text.

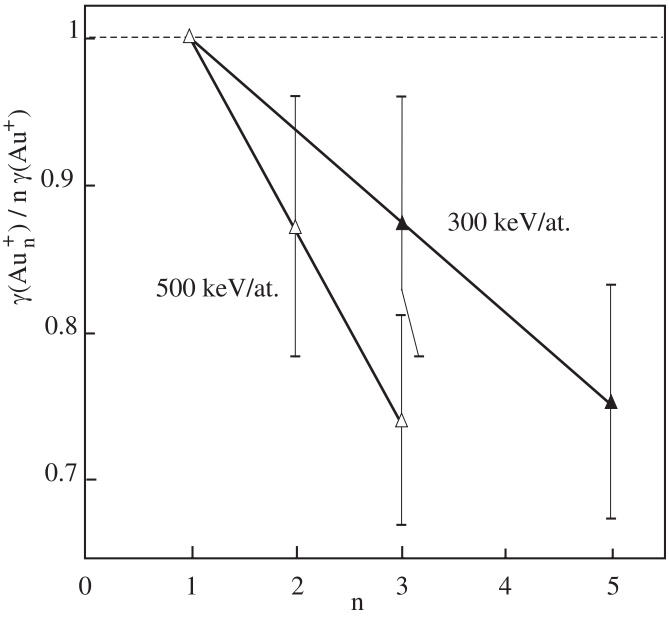

Fig. 3. Cluster size dependence of the ratio $\gamma(Au_n^+)/n\gamma(Au^+)$ for two cluster velocities.

with a high-intensity beam. The subsequent electron yield measurements with low-intensity beams did not reveal any dependence either on the number of incident ions or on the order in which the various (in energy and n value) incident beams were used. We can now compare the yields of a given target bombarded by various ions, which is the aim of our study.

We have studied the electron emission yield upon impact of monoatomic Au^+ ions, its dependence on the velocity, and its relation to the electronic energy loss rate S_e. We measured the electron emission from the entrance surface of the carbon foil (backward emission) at various incident energies between 300 keV and 2 MeV. The energy dependence of the measured yields γ_B is given in Fig. 2. These yields are shown to be proportional to the electronic energy loss rate $S_e(Au^+)$ of Au^+ ions in carbon. The proportionality coefficient Λ_B is found to be 8.4 ± 0.3 nm/keV if tabulated values of $S_e(Au^+)$ [6] and an evaporated carbon density of $1.7\,g/cm^3$ are used. Our experimental results show that the proportionality between electron yield and electronic energy loss, already evidenced by Rothard *et al.* [7] for various target materials and heavy ions at higher energies, is still valid for carbon target and gold ions at energies between 1 and 10 keV/u. Moreover, the γ_B expression for heavy ions given in [7] gives a Λ_B value of 5.9 nm/keV for our experimental conditions (45° tilt angle), which is in fairly good agreement with our experimental results; this indicates that their relation can be extended beyond their experimental range.

Secondary electron emission induced by Au_n^+ clusters ($n \leq 5$) has been measured for energies of 300 and 500 keV/at. If we compare $\gamma(Au_n^+)$, the electron yield induced by Au_n^+ cluster ions, with the product $n\gamma(Au^+)$, the electron yield of n independent Au^+ ions of the same velocity, the value of the ratio $\gamma(Au_n^+)/n\gamma(Au^+)$ will be different from unity if a cluster effect exists. The experimental values of this ratio, given in Fig. 3, clearly show that the Au atoms in a cluster do not interact independently from each other with target electrons. The ratio values are below unity and indicate a strong reduction of the electron yield per incident Au atom, the effect being stronger at higher velocity. It must be noted that for our experimental conditions, the interaction radius of a gold atom in amorphous carbon (the screening distance) is less than 1 Å, smaller than the mean interatomic distance in the incident cluster (≈ 2 Å), and that the projectile velocity is below the velocity threshold for plasmon excitation. Opposite velocity dependence of the cluster effect in carbon has been observed with H_n^+ cluster ions above this velocity threshold [8]. The low velocity Au_n^+ cluster effect does not depend strongly on the material, as has been similarly observed in insulating CsI targets in the 0.4–30 keV/u energy range [9]. Nevertheless, to explain the cluster effect on electron emission, it can be thought that the primary electron excitation is probably not the only emission step to be affected, and that the electron transport in the solid toward the surface is also highly modified in the impact area of the cluster.

4 Cluster effect on damage production in silicon crystal

In order to evidence a possible cluster effect in the processes of damage creation, we irradiated silicon crystals, at room temperature, with two kinds of projectiles of the same velocity: Au^+ single ions of 500 keV energy and Au_3^+

clusters of 1.5 MeV total energy. The targets used were cleaved from a p-type boron-doped silicon wafer of (100) orientation. The beam was electrically swept in order to ensure homogeneous implantation over an area of $\approx 1\,\mathrm{cm}^2$. In both cases, the irradiation fluence ranged from 10^{12} to $10^{14}\,\mathrm{at/cm}^2$. The beam current was periodically measured by the use of a Faraday cup set behind the target. Typical intensity values (for a beam diameter of 1 mm) were $\approx 20\,\mathrm{nA}$ and $\approx 8\,\mathrm{nA}$ for Au^+ and Au_3^+ projectiles, respectively.

The radiation-induced disorder was measured by means of Rutherford backscattering spectrometry in channeling geometry (RBS-C) with a 2 MeV $^4He^+$ beam delivered by the Van de Graaff accelerator of the Département de Physique des Matériaux de Lyon. In these measurements, we were able to measure the number of implanted gold atoms, check the gold irradiation fluence Φ, and measure the relative disorder α_0 at the Si surface. This latter parameter is given by the classical relation $\alpha_0 = (\chi_0 - \chi_v)/(1 - \chi_v)$, where χ_0 is the normalized-to-random Rutherford yield measured at the low-energy edge of the silicon surface peak, and χ_v is the same parameter measured on a virgin part of the silicon target (typically: $\chi_v = 2.5\%$).

For the two projectiles used (Au^+ and Au_3^+), the evolution of α_0 versus the fluence Φ (given in the number of single Au atoms per cm^2) is displayed in Fig. 4. In both cases, the radiation-induced disorder is necessarily ascribable to atomic displacements via elastic processes: (i) The nuclear energy loss rate S_n of Au atoms in silicon exceeds the electronic energy loss rate S_e by a factor of 4; from the computer code SRIM97 [6], $S_n = 3.2\,\mathrm{keV/nm}$ and $S_e = 0.9\,\mathrm{keV/nm}$ at the energy of 500 keV. (ii) The damage creation in silicon via inelastic processes, which has been recently evidenced for cluster irradiation [10], requires very large values of the electronic energy loss rate ($> 30\,\mathrm{keV/nm}$ at low projectile velocity) which are far from being reached in the present irradiation conditions.

The disorder kinetics related to Au^+ irradiations at 500 keV cannot be fitted by an exponential ($\alpha_0 = 1 - \exp(-A_d\Phi)$, where A_d is the damage cross section) derived from a direct impact model [11]. More refined scenarios have been proposed [12,13] to describe the fluence dependence of the disorder created by heavy ions in silicon. It must be noticed, however, that the critical dose Φ_c for a complete surface amorphization ($\Phi_c \approx 10^{14}\,\mathrm{at/cm}^2$ in the case of Au^+ bombardment, according to Fig. 4) agrees reasonably well with the value calculated from an SRIM simulation using a conventional displacement energy of 20 eV per silicon atom.

The more striking feature evidenced from Fig. 4 is the strong enhancement of defect production at the Si surface for Au_3^+ projectiles. For example, for a fluence of $2 \times 10^{13}\,\mathrm{at/cm}^2$, the surface damage induced by Au_3^+ clusters exceeds the surface damage induced by Au^+ single ions by a factor of between 2 and 3. In addition, the Φ_c value drops down to $\approx 5 \times 10^{13}\,\mathrm{at/cm}^2$ when the irradiation is performed with clusters. Such a nonlinear effect for defect creation in Si has already been pointed out by means of Ge_n^+ ($n \leq 3$) irradiations at an energy of 2.8 MeV per atom [14] and by fullerene irradiations at energies up to 530 keV [15]. Interestingly, the ion emission yields of CsI targets [16] and the sputtering yields of gold targets [17] bombarded with gold clusters exhibit also a nonlinear dependence on the cluster size. The thermal spike model for collisional sputtering [18] predicts at least an n^2 dependence of the sputtering yields on the cluster size. It would be worthwhile to check whether the thermal spike model can apply to the damage induced by high-density collision cascades following cluster bombardments.

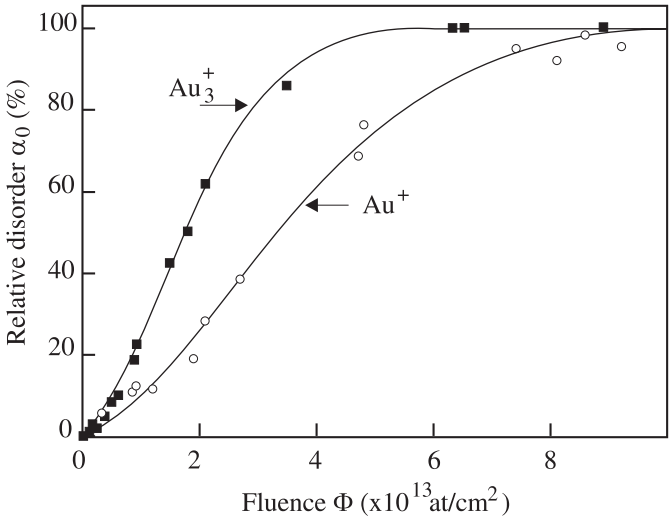

Fig. 4. Fluence dependence (in atoms per cm^2) of the relative disorder produced at the surface of a silicon crystal by Au^+ and Au_3^+ ions of energy 500 keV/at. The solid lines are to guide the eye.

5 Conclusion

The method of installing a LMIS source on the high-voltage terminal of single-stage electrostatic accelerators, as done in Lyon, is definitely the best for producing MeV gold cluster beams In addition to the performances of the LMIS sources, which are able to produce intense ion flux of pure metallic clusters and also bimetallic clusters from alloys, the high transmission of such accelerators leads to easy transport of the beams over distances of several meters and, after magnetic analysis, to intense beams of mass-selected clusters at the target site. The size range of accelerated gold clusters with beam currents above 10 pA, restricted up to now to small clusters ($n \leq 3$) on tandem accelerators, is extended with this experimental set-up to larger clusters up to Au_{13}^+. These intense cluster beams are particularly useful for irradiation experiments in studies of material modifications and surface sputtering induced by atomic collisions under cluster impact. The large cluster size range now available will allow us to study systematically the size dependences of the secondary electron emission and of the damage creation in crystals. Such studies should give essential information on the physical processes

that govern the electronic and nuclear interactions of energetic clusters in solids. Moreover, the impact of large clusters on solids at MeV energies could lead to spectacular surface modifications on a nanometric scale.

References

1. *Proceedings of the Conference on Polyatomic Ion Impact on Solids and Related Phenomena, Saint-Malo, 1993*, Nucl. Instrum. Methods, Phys. Res. B **88** (1994)
2. *Proceedings of the E-MRS'95 Conference on Correlated Effects in Atomic and Cluster Ion Bombardment and Implantation, Strasbourg, 1995*, Nucl. Instrum. Methods, Phys. Res. B **112** (1996)
3. P. Attal, S. Della-Negra, D. Gardès, J.D. Larson, Y. Le Beyec, R. Vienet-Legué, B. Waast: Nucl. Instrum. Methods, Phys. Res. A **328**, 293 (1993)
4. G. Lakits, F. Aumayr, H. Winter: Rev. Sci. Instrum. **60**, 3151 (1989)
5. Z. Vidovic: Thèse de Doctorat, University of Lyon-1 (1997)
6. J.F. Ziegler: SRIM97 computer code
7. H. Rothard, K. Kroneberger, A. Clouvas, E. Veje, P. Lorensen, N. Keller, J. Kemmler, W. Meckbach, K.O. Groeneveld: Phys. Rev. A **41**, 2521 (1990)
8. A. Billebaud, D. Dauvergne, M. Fallavier, R. Kirsch, J.C. Poizat, J. Remillieux, H. Rothard, J.P. Thomas: Nucl. Instrum. Methods, Phys. Res. B **112**, 79 (1996)
9. K. Baudin, A. Brunelle, S. Della-Negra, J. Depauw, Y. Le Beyec, E.S. Parilis: Nucl. Instrum. Methods, Phys. Res. B **117**, 47 (1996)
10. B. Canut, N. Bonardi, S.M.M. Ramos, S. Della-Negra: Nucl. Instrum. Methods, Phys. Res. B **146**, 296 (1998)
11. J.F. Gibbons: *Proceedings of IEEE* **60**, 1062 (1972)
12. N. Hecking, K.F. Heidemann, E. Te Kaat: Nucl. Instrum. Methods, Phys. Res. B **15**, 760 (1986)
13. S.U. Campisano, S. Coffa, V. Raineri, F. Priolo, E. Rimini: Nucl. Instrum. Methods, Phys. Res. B **80/81**, 514 (1993)
14. M. Döbeli, F. Ames, R.M. Ender, M. Suter, H.A. Synal, D. Vetterli: Nucl. Instrum. Methods, Phys. Res. B **106**, 43 (1995)
15. Hao Shen, C. Brink, P. Hvelplund, S. Shiryaev, Pei Xiong Shi, J.A. Davies: Nucl. Instrum. Methods, Phys. Res. B **129**, 203 (1997)
16. Y. Le Beyec: Int. J. Mass Spectrom. Ion Processes **174**, 101 (1998)
17. H.H. Andersen, A. Brunelle, S. Della-Negra, J. Depauw, D. Jacquet, Y. Le Beyec, J. Chaumont, H. Bernas: Phys. Rev. Lett. **80**, 5433 (1998)
18. P. Sigmund, C. Claussen: J. Appl. Phys. **52**, 990 (1981)